AIMS Mathematics, 9(3): 6281–6304.
DOI: 10.3934/math.2024306
Received: 18 December 2023
Revised: 18 January 2024
Accepted: 26 January 2024
Published: 04 February 2024

http://www.aimspress.com/journal/Math

Research article

A mathematical model for predicting and controlling COVID-19 transmission with impulsive vaccination

Chontita Rattanakul[1,2] **and Inthira Chaiya**[3,*]

[1] Department of Mathematics, Faculty of Science, Mahidol University, Bangkok 10400, Thailand
[2] Centre of Excellence in Mathematics, MHESI, Bangkok 10400, Thailand
[3] Department of Mathematics, Faculty of Science, Mahasarakham University, Mahasarakham 44150, Thailand

* **Correspondence:** Email: inthira.c@msu.ac.th; Tel: +6643754247; Fax: +6643754247.

Abstract: This study examines an epidemiological model known as the susceptible-exposed-infected-hospitalized-recovered (SEIHR) model, with and without impulsive vaccination strategies. First, the model was analyzed without impulsive vaccination in the presence of a reinfection effect. Subsequently, it was studied as part of a periodic impulsive vaccination strategy targeting the susceptible population. These vaccination impulses were administered in very brief intervals at specific time instants, with a fixed time gap between each impulse. The two approaches can be modified to respond to different amounts of susceptibility, with control efforts intensifying as susceptibility levels rise. The model's analysis includes crucial aspects such as the non-negativity of solutions, the existence of steady states, and the stability corresponding to the basic reproduction number. We demonstrate that when vaccination measures are taken into account, the basic reproduction number remains as less than one. Therefore, the disease-free equilibrium in the case of vaccination could still be asymptotically stable at the higher disease transmission rate, as compared to the case of no vaccination in which the disease-free equilibrium may no longer be asymptotically stable. Furthermore, we show that when the disease-free equilibrium is stable, the endemic equilibrium cannot be attained, and that when the reproduction number rises above unity, the disease-free equilibrium becomes unstable while the endemic equilibrium becomes stable. We have also derived conditions for the global stability of both equilibriums. To support our theoretical results, we have constructed a time series of numerical simulations and compared them with real-world data from the ongoing SARS-CoV-2 (COVID-19) pandemic.

Keywords: mathematical model; periodic impulsive vaccination; COVID-19; epidemic model; stability
Mathematics Subject Classification: 34A34, 34A37, 34D23, 37G15, 92-10

1. Introduction

COVID-19, first identified in Wuhan, China in December 2019, has become a global health crisis with severe implications [31]. Stemming from a genetic mix between bat and cobra coronaviruses, this novel virus swiftly transcended species boundaries, leading to a surge in cases and fatalities worldwide. The World Health Organization (WHO) officially declared it a pandemic, necessitating urgent research efforts. As of the time of the report of the latest data from the WHO [1], there have been 5,304,772 confirmed cases and 342,029 deaths globally, accompanied by substantial economic repercussions. The imperative to understand and manage COVID-19's transmission dynamics has fueled extensive research, with mathematical modeling serving as a pivotal tool [6, 8, 14, 29].

The COVID-19 pandemic has prompted the classification of populations into various categories: susceptible, exposed, symptomatic, asymptomatic, quarantined, and recovered. Vaccines have emerged as a pivotal resource in our battle against COVID-19. While these vaccines have been developed relatively recently, the available data so far are varied. Notably, recent analyses suggest a decline in protection against reinfection to 41% after 12 months, particularly for individuals with both prior infection and vaccination [2]. It is important to acknowledge that this result may raise concerns among those seeking long-lasting protection against COVID-19.

In the realm of epidemiology, models such as the SIR and SEIR models offer simplified frameworks for analysis [10, 12, 17]. Numerous COVID-19 models have been proposed and modified to provide insights into the pandemic's progression. For example, Kuga and Tanimoto [18] explored the efficacy of imperfect vaccination and defense against contagion, comparing partial immunity through vaccination and contagion defense. Their findings within the analytical framework revealed a marginally superior outcome for imperfect vaccination. Lin et al. [21] introduced an SEIR model that accounts for susceptible, exposed, infected, and removed individuals. Anastassopoulou et al. [5] incorporated a death compartment into an SIR model to better reflect COVID-19 dynamics. Casella [9] considered delayed effects in the SIR model, while Wu et al. [32] assessed COVID-19 severity through transmission dynamics. Recently, Singh et al. [24] studied the emergence of COVID-19 in India, as well as the imposition and subsequent easing of lockdown measures, and they proposed a variable-order fractional SIR model for predicting COVID-19 cases at the state level, including a parameter for testing and quarantine.

Optimal control strategies have proven effective in managing epidemic outbreaks [16, 26]. This approach aims to minimize infection rates while optimizing the costs of treatment and prevention [25, 27, 28]. Interventions may encompass treatments, vaccines, or social distancing measures. Park and Kim [22] utilized a susceptible-infected-susceptible model to analyze the basic reproduction number in South Korea, aiding in the determination of vaccine stockpile requirements for achieving herd immunity. Etxeberria-Etxaniz et al. [15] investigated a model of SEIR outbreak with demography and impulsive vaccination, focusing on the effects of periodic vaccination and newborns for susceptible individuals. Recently, Alazman et al. [4] introduced a restricted SIR model for analyzing COVID-19 dynamics, emphasizing its ability to depict multiple disease waves and assess the vaccination's impact.

Impulsive control introduces a targeted and well-timed approach to vaccinations, deviating from continuous vaccination strategies. This deviation allows individuals to receive booster shots periodically, aligning with the natural ebb and flow of their immunity. This approach offers distinct

advantages, including the optimization of resource utilization, reduction in infection rates, and adaptability to changing dynamics.

Our proposed mathematical model explicitly incorporates impulsive control as a crucial component. Within this model, we account for susceptible, exposed, infected, hospitalized, vaccinated, and recovered individuals, providing a comprehensive representation of the intricate dynamics of COVID-19. The impulsive vaccination in our model mirrors the strategic administration of vaccines at specific time points, adding a layer of precision and effectiveness to control efforts.

2. Mathematical model

To comprehensively investigate the effects of controlling the epidemic through impulsive vaccination, we propose a novel mathematical model for the transmission of COVID-19. This model incorporates six distinct population classes: the susceptible class (S), the vaccinated class (V), the exposed class (E), the infected class (I), the hospitalized class (H), and the recovered class (R).

The susceptible class (S) represents individuals who are at risk of contracting the virus. These individuals are recruited into this category at a rate denoted by Λ. The model accounts for the COVID-19 mortality rate (δ_1) and the mortality rate during hospitalization (δ_2). Furthermore, the natural death rate (μ) is applicable to all six classes, reflecting the expected mortality in the absence of the virus. The transmission of the virus within the population is governed by the transmission rate (β), which quantifies how easily the virus spreads. The progression rate from the exposed class (E) to the infected class (I) is represented by ρ. Additionally, the model considers the rate (α) at which infected individuals transition from the infectious class to the hospitalized class (H). Individuals in the infected and hospitalized classes have the potential for recovery, occurring at rates denoted by q and κ, respectively. Moreover, the model accounts for individuals moving from the vaccinated and recovered classes back to the susceptible class upon losing their immunity. These transitions are determined by the rates ω and ϕ. Crucially, the model incorporates the impact of impulsive vaccination on susceptible individuals. They receive vaccinations and may receive booster shots when their immunity wanes, occurring at a rate represented by γ, in a periodic manner with a period of T. In summary, our model is described by a system of impulsive ordinary differential equations as follows: For $t \neq nT$,

$$\begin{aligned}
\frac{dS}{dt} &= \Lambda - \beta S I - \mu S + \phi R + \omega V,\\
\frac{dV}{dt} &= -(\omega + \mu)V,\\
\frac{dE}{dt} &= \beta S I - (\rho + \mu)E,\\
\frac{dI}{dt} &= \rho E - (q + \delta_1 + \alpha + \mu)I,\\
\frac{dH}{dt} &= \alpha I - (\kappa + \delta_2 + \mu)H,\\
\frac{dR}{dt} &= qI + \kappa H - (\phi + \mu)R.
\end{aligned} \tag{2.1}$$

For $t = nT$,

$$\begin{aligned} S(nT^+) &= (1-\gamma)S(nT), \\ V(nT^+) &= V(nT) + \gamma S(nT), \\ E(nT^+) &= E(nT), \\ I(nT^+) &= I(nT), \\ H(nT^+) &= H(nT), \\ R(nT^+) &= R(nT), \end{aligned} \tag{2.2}$$

where T denotes the period between two subsequent vaccinations, $n \in \mathbb{Z}_+, \mathbb{Z}_+ = 1, 2, 3, ...$, and γ represents flow from the susceptible class to the vaccinated class, $0 < \gamma < 1$. The notation $S(nT^+)$ represents the right limit of $S(t)$ as t approaches nT (i.e., the value after accounting for the impulse). At impulsive time instants, susceptible individuals who are removed become vaccinated, denoted as $V(nT^+) = V(nT) + \gamma S(nT)$.

A diagram of the impulsive vaccination model of COVID-19 for the systems (2.1) and (2.2) are as illustrated in Figure 1.

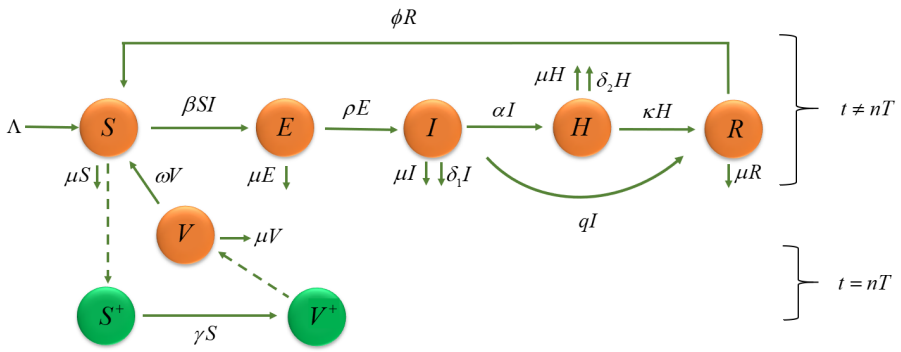

Figure 1. Diagram of the impulsive vaccination model of COVID-19.

3. Dynamics of the model without vaccination

Now, we examine the simplified system in the absence of vaccination.

$$\begin{aligned} \frac{dS}{dt} &= \Lambda - \beta S I - \mu S + \phi R, \\ \frac{dE}{dt} &= \beta S I - (\rho + \mu)E, \\ \frac{dI}{dt} &= \rho E - (q + \delta_1 + \alpha + \mu)I, \\ \frac{dH}{dt} &= \alpha I - (\kappa + \delta_2 + \mu)H, \\ \frac{dR}{dt} &= qI + \kappa H - (\phi + \mu)R. \end{aligned} \tag{3.1}$$

3.1. Existence of the solution

Lemma 3.1. *(Derrick and Grossman theorem [13]) Let* Ω *denote the following region:*

$$|t - t_0| \leq a\,,\ \|u - u_0\| \leq 1,\ u = (u_1, u_2,\ \ldots,\ u_n), u_0 = (u_{10}, u_{20},\ \ldots,\ u_{n0})\,,$$

and suppose that $f(t, u)$ *satisfies the Lipchitz condition given by*

$$\|f(t, u_1) - f(t, u_2)\| \leq k\|u_1 - u_2\|,$$

whenever the pairs (t, u_1) *and* (t, u_2) *belong to* Ω*, where* k *is a positive constant. Then, there is a constant* $a \geq 0$ *such that there exists a unique continuous vector solution of* $u(t)$ *of the system in the interval* $t - t_0 \leq a$*.*

It is important to note that the condition is satisfied by the requirement that $\partial f_i/\partial u_j$ *for* i, $j = 1, 2, 3, \ldots, n$ *is continuous and bounded in* Ω*.*

Theorem 3.1. *The solution of the model* (3.1) *with the initial conditions* $S(0) \geq 0, E(0) \geq 0, I(0) \geq 0$, $H(0) \geq 0$, *and* $R(0) \geq 0$ *exists and is unique in* $\mathbb{R}^5_+$ *for all* $t \geq 0$*.*

Proof. The following can be used to express the right-hand sides of system (3.1)

$$\begin{aligned}
f_1 &= \Lambda - \beta S I - \mu S + \phi R,\\
f_2 &= \beta S I - (\rho + \mu)E,\\
f_3 &= \rho E - (q + \delta_1 + \alpha + \mu)I,\\
f_4 &= \alpha I - (\kappa + \delta_2 + \mu)H,\\
f_5 &= qI + \kappa H - (\phi + \mu)R.
\end{aligned}$$

It is reasonable to show that $\partial f_i/\partial u_i$ is continuous and $|\partial f_i/\partial u_i| < \infty$ for $i, j = 1, 2, \ldots, 5$, where $u_1 = S, u_2 = E, u_3 = I, u_4 = H$, and $u_5 = R$. According to Lemma 3.1, the system (3.1) has a unique solution.

3.2. Invariant region

Let $N(t)$ be the total number of human populations at time t. It follows that

$$\begin{aligned}
\frac{dN}{dt} &= \frac{dS}{dt} + \frac{dE}{dt} + \frac{dI}{dt} + \frac{dH}{dt} + \frac{dR}{dt}\\
&= \Lambda - \mu N - \delta_1 I - \delta_2 H.
\end{aligned}$$

Then,

$$\lim_{\sup t \to \infty} N \leq \frac{\Lambda}{\mu}.$$

As a result, the possible region for the system (3.1) is given by

$$\Omega = \left\{(S, E, I, H, R) \in \mathbb{R}^5 : S \geq 0, E \geq 0, I \geq 0, H \geq 0, R \geq 0, N \leq \frac{\Lambda}{\mu}\right\}.$$

3.3. Positivity of the solution

Theorem 3.2. *The solution of the system* (3.1) *with the initial conditions* $S(0) \geq 0, E(0) \geq 0, I(0) \geq 0$, $H(0) \geq 0$, *and* $R(0) \geq 0$ *is positive in* $\mathbb{R}^5$ *for all* $t \geq 0$.

Proof. Positivity of $S(t)$: In the first equation of system (3.1), expressed as $dS/dt = \Lambda - \beta S I - \mu S + \phi R$, we can establish an inequality without loss of generality: $dS/dt \geq -(\beta\Lambda + \mu^2)S/\mu$. Employing the separation of variables method and integration, the solution is as follows: $S(t) \geq S(0)\exp[-(\beta\Lambda + \mu^2)t/\mu]$. Consequently, we can confidently assert that $S(t) \geq 0$.

Furthermore, by applying the same rigorous procedure, we can establish the positivity of other variables within the system. Consequently, we can confidently assert that the solutions of the model system (3.1) maintain non-negativity for all time intervals $t \geq 0$.

3.4. Equilibria

There are two equilibria, as articulated below:

(i) The disease-free equilibrium:

$$EE = (S^0, E^0, I^0, H^0, R^0) = \left(\frac{\Lambda}{\mu}, 0, 0, 0, 0\right),$$

(ii) The endemic equilibrium:

$$EE^* = (S^*, E^*, I^*, H^*, R^*),$$

where

$$S^* = \frac{AB}{\beta\rho},$$

$$E^* = \frac{\mu A^2 BCD\left(\frac{\Lambda\beta\rho}{\mu AB} - 1\right)}{\beta\rho[\mu A(C+\rho)(D+\mu) + \mu BC(D+\mu) + \rho\phi((\delta_1+\mu)(D+\mu) + \alpha(\delta_2+2\mu))]},$$

$$I^* = \frac{\mu ABCD\left(\frac{\Lambda\beta\rho}{\mu AB} - 1\right)}{\beta[\mu A(C+\rho)(D+\mu) + \mu BC(D+\mu) + \rho\phi((\delta_1+\mu)(D+\mu) + \alpha(\delta_2+2\mu))]},$$

$$H^* = \frac{\mu\alpha ABC\left(\frac{\Lambda\beta\rho}{\mu AB} - 1\right)}{\beta[\mu A(C+\rho)(D+\mu) + \mu BC(D+\mu) + \rho\phi((\delta_1+\mu)(D+\mu) + \alpha(\delta_2+2\mu))]},$$

$$R^* = \frac{\mu AB(qD + \alpha\kappa)\left(\frac{\Lambda\beta\rho}{\mu AB} - 1\right)}{\beta[\mu A(C+\rho)(D+\mu) + \mu BC(D+\mu) + \rho\phi((\delta_1+\mu)(D+\mu) + \alpha(\delta_2+2\mu))]},$$

with $A = q + \delta_1 + \alpha + \mu$, $B = \rho + \mu$, $C = \phi + \mu$, $D = \delta_2 + \kappa + \mu$.

3.5. The basic reproduction number (R_0)

In accordance with the insights provided by van den Driessche and Watmough [30], we proceed to ascertain the basic reproduction number, denoted as R_0. This parameter signifies the number of new

infectious cases generated by a single infectious individual when all individuals within the population are in the susceptible class. To achieve this, we employ the established next-generation matrix method for analysis. Within this method, we define matrices as follows:

$$f = \begin{pmatrix} \beta S I \\ 0 \end{pmatrix}, v = \begin{pmatrix} BE \\ AI - \rho E \end{pmatrix}.$$

Then, the following F and V are respectively obtained by utilizing the Jacobian matrices of f and v:

$$F = \begin{pmatrix} 0 & \beta S^0 \\ 0 & 0 \end{pmatrix}, V = \begin{pmatrix} B & 0 \\ -\rho & A \end{pmatrix},$$

Additionally, we can write

$$FV^{-1} = \begin{pmatrix} \frac{\beta\rho S^0}{AB} & \frac{\beta S^0}{A} \\ 0 & 0 \end{pmatrix}.$$

The eigenvalues of FV^{-1} are given by

$$\lambda_1 = 0 \text{ and } \lambda_2 = \frac{\Lambda\beta\rho}{\mu AB}.$$

Therefore, the basic reproduction number is defined as

$$R_0 = \frac{\beta\rho S^0}{(q + \delta_1 + \alpha + \mu)(\rho + \mu)} = \frac{\Lambda\beta\rho}{\mu AB}.$$

We can interpret R_0 as follows:

$\beta S I$ represents the daily number of susceptible individuals infected by infected individuals. Therefore, the daily number of susceptible individuals infected by one infected individual is βS, and the average duration of infection is $\frac{1}{q+\delta_1+\alpha+\mu}$. Exposed individuals develop into infected individuals with the proportion $\frac{\rho}{\rho+\mu}$. Thus, $R_0 = \frac{\beta\rho S^0}{(q+\delta_1+\alpha+\mu)(\rho+\mu)}$ represents the average number of susceptible individuals infected by one infected individual.

3.6. The local stability of the disease-free equilibrium

Theorem 3.3. *The disease-free equilibrium* $EE = (S^0, E^0, I^0, H^0, R^0) = \left(\frac{\Lambda}{\mu}, 0, 0, 0, 0\right)$ *is locally asymptotically stable if* $R_0 < 1$.

Proof. The Jacobian matrix of the system (3.1) at EE is calculated as follows:

$$J(EE) = \begin{pmatrix} -\mu & 0 & -\beta S^0 & 0 & \phi \\ 0 & -B & \beta S^0 & 0 & 0 \\ 0 & \rho & -A & 0 & 0 \\ 0 & 0 & \alpha & -D & 0 \\ 0 & 0 & q & \kappa & -C \end{pmatrix}.$$

Setting $\det(J(EE) - \eta I) = 0$, we have the following eigenvalues:

$$\eta_1 = -\mu, \eta_2 = -C, \eta_3 = -D,$$

and the roots of the following equation:

$$\eta^2 + (A + B)\eta + AB(1 - R_0) = 0. \tag{3.2}$$

We establish a strong guarantee that all roots of Eq (3.2) have a negative real component when $R_0 < 1$ by employing the Routh-Hurwitz criteria. As a result, we conclude that the equilibrium point indicated as EE exhibits local asymptotic stability when $R_0 < 1$, which corresponds to our intended conclusion.

3.7. The local stability of the endemic equilibrium

Theorem 3.4. *The endemic equilibrium point $EE^* = (S^*, E^*, I^*, H^*, R^*)$ is stable whenever it exists.*

Proof. We rewrite the endemic equilibrium point $EE^* = (S^*, E^*, I^*, H^*, R^*)$ as follows:

$$\begin{aligned}
S^* &= \frac{\Lambda}{\mu R_0},\\
E^* &= \frac{\mu A^2 BCD\,(R_0 - 1)}{\beta\rho[\mu A(C + \rho)(D + \mu) + \mu BC(D + \mu) + \rho\phi((\delta_1 + \mu)(D + \mu) + \alpha(\delta_2 + 2\mu))]},\\
I^* &= \frac{\mu ABCD\,(R_0 - 1)}{\beta[\mu A(C + \rho)(D + \mu) + \mu BC(D + \mu) + \rho\phi((\delta_1 + \mu)(D + \mu) + \alpha(\delta_2 + 2\mu))]},\\
H^* &= \frac{\mu\alpha ABC\,(R_0 - 1)}{\beta[\mu A(C + \rho)(D + \mu) + \mu BC(D + \mu) + \rho\phi((\delta_1 + \mu)(D + \mu) + \alpha(\delta_2 + 2\mu))]},\\
R^* &= \frac{\mu AB(qD + \alpha\kappa)\,(R_0 - 1)}{\beta[\mu A(C + \rho)(D + \mu) + \mu BC(D + \mu) + \rho\phi((\delta_1 + \mu)(D + \mu) + \alpha(\delta_2 + 2\mu))]},
\end{aligned}$$

Note that EE^* exists if all components are positive, that is, $R_0 > 1$. Next, the Jacobian matrix of the system (3.1) at the endemic equilibrium can be obtained as follows:

$$J(EE^*) = \begin{pmatrix}
-\beta I^* - \mu & 0 & -\beta S^* & 0 & \phi\\
\beta I^* & -B & \beta S^* & 0 & 0\\
0 & \rho & -A & 0 & 0\\
0 & 0 & \alpha & -D & 0\\
0 & 0 & q & \kappa & -C
\end{pmatrix}.$$

Setting $\det(J(EE^*) - \zeta I) = 0$, we have the characteristic equation

$$\zeta^5 + a_4\zeta^4 + a_3\zeta^3 + a_2\zeta^2 + a_1\zeta + a_0 = 0. \tag{3.3}$$

where

$$\begin{aligned}
a_4 \equiv&\beta I^* + A + B + C + D + \mu,\\
a_3 \equiv&\beta(A + B + C + D)I^* + (A + B)(C + D) + CD + \mu(A + B + C + D),\\
a_2 \equiv&\beta((A + B)(C + D) + AB + CD)I^* + \mu((A + B)(C + D) + CD) + CD(A + B),\\
a_1 \equiv&\beta(CD(A + B) + ABD + BC(\delta_1 + \alpha + \mu) + q\mu(C + \rho))I^* + \mu CD(A + B),\\
a_0 \equiv&\beta(BCD(\delta_1 + \mu) + \alpha BC(\delta_2 + \mu) + \alpha\kappa\mu(C + \rho) + q\mu(C + \rho))I^*.
\end{aligned}$$

Note that $a_i > 0$ for $i = 0, 1, ..., 4$ if $I^* > 0$ i.e., $R_0 > 1$. Using the Routh-Hurwitz criteria, we can ensure that all roots of the given equation have a negative real component by applying the following:

$$a_4 > 0, a_3 > 0, a_2 > 0, a_1 > 0, a_0 > 0, a_3a_4 > a_2, a_2a_3a_4 > a_1a_4^2 + a_2^2,$$

$$a_1a_2a_3a_4 + 2a_0a_1a_4 + a_0a_2a_3 > a_1^2a_4^2 + a_0a_3^2a_4 + a_1a_3^2 + a_0^2.$$

As a result, $R_0 > 1$. Therefore, EE^* is locally asymptotically stable whenever it exists, as is the intended conclusion.

3.8. The global stability of the disease-free equilibrium

Theorem 3.5. *The disease-free equilibrium* $EE = (S^0, E^0, I^0, H^0, R^0) = \left(\frac{\Lambda}{\mu}, 0, 0, 0, 0\right)$ *is globally asymptotically stable if* $R_0 < 1$.

Proof. To prove the global asymptotic stability of the disease-free equilibrium, we employ the method of applying the Lyapunov function. Systematically, we define a Lyapunov function L such that

$$L = \rho E + BI.$$

Then,

$$\begin{aligned}\frac{dL}{dt} &= \rho\frac{dE}{dt} + B\frac{dI}{dt}\\ &= \rho\left[\beta S I - BE\right] + B\left[\rho E - AI\right]\\ &= AB(R_0 - 1)I.\end{aligned}$$

So, $dL/dt \leq 0$ if $R_0 < 1$. Furthermore, $dL/dt = 0$ if $I = 0$ or $R_0 = 1$. From this, we see that $EE = (S^0, E^0, I^0, H^0, R^0) = \left(\frac{\Lambda}{\mu}, 0, 0, 0, 0\right)$ is the only singleton in $\{(S^0, E^0, I^0, H^0, R^0) \in \Omega : dL/dt = 0\}$. Therefore by the principle of LaSalle [19], EE is globally asymptotically stable if $R_0 < 1$.

3.9. The global stability of the endemic equilibrium

Theorem 3.6. *The endemic equilibrium point* $EE^* = (S^*, E^*, I^*, H^*, R^*)$ *exists and is globally asymptotically stable if* $R_0 > 1$ *and* $m < n$.

Proof. The Lyapunov function is used to demonstrate the global asymptotic stability of the endemic equilibrium. We define the Lyapunov function L as follows:

$$\begin{aligned}L(S^*, E^*, I^*, H^*, R^*) = &\left(S - S^* \ln\frac{S}{S^*}\right) + \left(E - E^* \ln\frac{E}{E^*}\right) + \left(I - I^* \ln\frac{I}{I^*}\right)\\ &+ \left(H - H^* \ln\frac{H}{H^*}\right) + \left(R - R^* \ln\frac{R}{R^*}\right).\end{aligned}$$

Note that EE^* exists if $R_0 > 1$. By directly calculating the derivative of L along the system (3.1), we obtain

$$\frac{dL}{dt} = \left(1 - \frac{S^*}{S}\right)\frac{dS}{dt} + \left(1 - \frac{E^*}{E}\right)\frac{dE}{dt} + \left(1 - \frac{I^*}{I}\right)\frac{dI}{dt} + \left(1 - \frac{H^*}{H}\right)\frac{dH}{dt} + \left(1 - \frac{R^*}{R}\right)\frac{dR}{dt}$$

$$= \left(1 - \frac{S^*}{S}\right)[\Lambda - \beta S I - \mu S + \phi R] + \left(1 - \frac{E^*}{E}\right)[\beta S I - BE] + \left(1 - \frac{I^*}{I}\right)[\rho E - AI]$$
$$+ \left(1 - \frac{H^*}{H}\right)[\alpha I - DH] + \left(1 - \frac{R^*}{R}\right)[qI + \kappa H - CR]$$
$$= -(\Lambda + \phi R)\left(\frac{S^*}{S} - 1\right) - \beta I\left(\frac{S E^*}{E} - S^*\right) - \rho E\left(\frac{I^*}{I} - 1\right) - \alpha I\left(\frac{H^*}{H} - 1\right)$$
$$- (qI + \kappa H)\left(\frac{R^*}{R} - 1\right) - \mu(S - S^*) - B(E - E^*) - A(I - I^*) - D(H - H^*) - C(R - R^*).$$

If $S = S^*, E = E^*, I = I^*, H = H^*$, and $R = R^*$, then $dL/dt = 0$.

By combining positive and negative terms, we get

$$\frac{dL}{dt} = m - n.$$

Here,

$$m \equiv \Lambda + \beta I S^* + \mu S^* + BE^* + AI^* + DH^* + CR^* + \phi R + \rho E + \alpha I + qI + \kappa H,$$
$$n \equiv \frac{\Lambda S^*}{S} + \frac{\phi R S^*}{S} + \frac{\beta S I E^*}{E} + \frac{\rho E I^*}{I} + \frac{\alpha I H^*}{H} + \frac{qI R^*}{R} + \frac{\kappa H R^*}{R} + \mu S + BE + AI + DH + CR.$$

Thus, if $m < n$, then $dL/dt \leq 0$. Furthermore, $dL/dt = 0$ if and only if $S = S^*, E = E^*, I = I^*, H = H^*$, and $R = R^*$. Consequently, the greatest compact invariant set in $\{(S^*, E^*, I^*, H^*, R^*) \in \Omega : dL/dt = 0\}$ is the singleton EE^*, representing the endemic equilibrium of the system (3.1). According to LaSalle's invariant principle [19], EE^* exists and is globally asymptotically stable in Ω if $R_0 > 1$ and $m < n$.

4. SEIHR model with impulsive vaccination

4.1. Preliminaries

Let

$$G : \mathbb{R}_+ \times \mathbb{R}_+^6 \to \mathbb{R}_+,$$

where $\mathbb{R}_+ = [0, \infty)$ and $\mathbb{R}_+^6 = \{X \in \mathbb{R}^6 : X = (S, V, E, I, H, R), S \geq 0, V \geq 0, E \geq 0, I \geq 0, H \geq 0, R \geq 0\}$. The map defined by the right-hand side of system (2.1) is denoted by $F = (F_1, F_2, ..., F_6)$.

Definition 4.1. *[7] The function G is said to belong to class G_0 if G is continuous in $(nT, (n+1)T] \times \mathbb{R}_+^6 \to \mathbb{R}_+$ and, for each $X \in \mathbb{R}_+^6, n \in \mathbb{Z}_+$,*

$$\lim_{(t,Y)\to(nT^+,X)} G(t, Y) = G(nT^+, X)$$

exists and is locally Lipschitzian in X.

Suppose that $G \in G_0$. For $t \in (nT, (n+1)T] \times \mathbb{R}_+^6$, the upper-right derivative of $G(t, X)$ in consideration of systems (2.1) *and* (2.2) *is defined by*

$$D^+G(t, X) = \limsup_{h\to 0^+} \frac{1}{h}[G(t + h, X + hF(t, X)) - G(t, X)].$$

The solution of systems (2.1) and (2.2), $X(t) = (S, V, E, I, H, R)$, is assumed to be a piecewise continuous function. It means that $X(t) : \mathbb{R}_+ \to \mathbb{R}_+^6, X(t)$ is continuous on $(nT, (n+1)T]$, $n \in \mathbb{Z}_+$ and $\lim_{t\to nT^+} X(t) = X(nT^+)$ exists. Therefore, the smoothness properties of F ensure the existence and uniqueness of a solution to systems (2.1) and (2.2) [20].

Lemma 4.1. *Suppose that* $X(t) = (S(t), V(t), E(t), I(t), H(t), R(t))$ *is a solution of the systems* (2.1) *and* (2.2) *with the initial value* $X(0^+) \geq 0$. *Then the solution* $X(t) \geq 0$ *for all* $t \geq 0$.

Proof. For $t \neq nT$, $dS/dt > 0$ whenever $S(t) = 0$. This implies that $S(t)$ is associated with a non-negative solution.

For $t = nT$, $S(nT^+) = (1-\gamma)S(nT)$. We can conclude that $S(t)$ remains non-negative, given that $S(nT) \geq 0$ (as established in the case that $t \neq nT$) and $0 < \gamma < 1$.

The same approach can be employed to demonstrate the non-negativity of $V(t), E(t), I(t), H(t)$, and $R(t)$. Thus, the proof is complete.

4.2. The epidemic model under periodic impulsive vaccination

By setting the time derivatives of system (2.1) to zero, applying the simultaneous conditions of zero values for both exposed and infectious compartments, and further requiring that the hospitalized and recovered compartments remain at zero, we obtain the disease-free steady-state as follows:

$$\begin{aligned}
S_{0*}^+ &= \lim_{n\to\infty} S(nT^+) = \frac{\Lambda(1-\gamma)(1-e^{-(\omega+\mu)T})}{\mu[1-(1-\gamma)e^{-(\omega+\mu)T}]},\\
S_{0*} &= \lim_{n\to\infty} S(nT) = \frac{S_{0*}^+}{1-\gamma} = \frac{\Lambda(1-e^{-(\omega+\mu)T})}{\mu[1-(1-\gamma)e^{-(\omega+\mu)T}]},\\
V_{0*}^+ &= N_{0*} - S_{0*}^+ = \frac{\Lambda\gamma}{\mu[1-(1-\gamma)e^{-(\omega+\mu)T}]},\\
V_{0*} &= N_{0*} - S_{0*} = \frac{\Lambda\gamma e^{-(\omega+\mu)T})}{\mu[1-(1-\gamma)e^{-(\omega+\mu)T}]},
\end{aligned}$$

where $E_{0*}^+ = E_{0*} = I_{0*}^+ = I_{0*} = H_{0*}^+ = H_{0*} = R_{0*}^+ = R_{0*} = 0$.

To analyze the dynamics of the impulsive vaccination, we initially examine the susceptible-vaccine subsystem at $(E = I = H = R = 0)$.

For $t \neq nT$,

$$\frac{dS}{dt} = \Lambda - \mu S + \omega V, \tag{4.1}$$

$$\frac{dV}{dt} = -(\omega+\mu)V. \tag{4.2}$$

For $t = nT$,

$$S(nT^+) = (1-\gamma)S(nT), \tag{4.3}$$

$$V(nT^+) = V(nT) + \gamma S(nT), \tag{4.4}$$

$$S(0^+) = S_0 \tag{4.5}$$

$$V(0^+) = V_0. \tag{4.6}$$

The systems given by Eqs (4.1)–(4.4) yield a periodic solution:

$$\tilde{S}(t) = \frac{\Lambda}{\mu}\left(1 - \frac{\gamma e^{-(\omega+\mu)(t-nT)}}{1-(1-\gamma)e^{-(\omega+\mu)T}}\right), \tilde{V}(t) = \frac{\Lambda\gamma e^{-(\omega+\mu)(t-nT)}}{\mu\left(1-(1-\gamma)e^{-(\omega+\mu)T}\right)},$$

with the initial conditions $\tilde{S}(0^+) = \frac{\Lambda}{\mu}\left(1 - \frac{\gamma}{1-(1-\gamma)e^{-(\omega+\mu)T}}\right) > 0$, $\tilde{V}(0^+) = \frac{\Lambda\gamma}{\mu\left(1-(1-\gamma)e^{-(\omega+\mu)T}\right)} > 0$ for $t \in (nT, (n+1)T], \forall n \in \mathbb{Z}_+$.

Therefore, the positive solution of Eqs (4.1)–(4.6) is given by

$$S(t) = \left(S_0 - \frac{\Lambda}{\mu}\left(1 - \frac{\gamma}{1-(1-\gamma)e^{-(\omega+\mu)T}}\right)\right)e^{-(\omega+\mu)t} + \tilde{S}(t), t \in (nT, (n+1)T],$$

$$V(t) = \left(V_0 - \frac{\Lambda\gamma}{\mu\left(1-(1-\gamma)e^{-(\omega+\mu)T}\right)}\right)e^{-(\omega+\mu)t} + \tilde{V}(t), t \in (nT, (n+1)T].$$

Lemma 4.2. *Equations* (4.1)–(4.6) *have a positive periodic solution* $(\tilde{S}(t), \tilde{V}(t))$, *and* $(S(t), V(t)) \to (\tilde{S}(t), \tilde{V}(t))$ *as* $t \to \infty$ *for every solution* $(S(t), V(t))$.

Therefore, the periodic solution of the systems (2.1) and (2.2) in the absence of E, I, H, and R is given by

$$(\tilde{S}(t), \tilde{V}(t), 0, 0, 0, 0) = \left(\frac{\Lambda}{\mu}\left(1 - \frac{\gamma e^{-(\omega+\mu)(t-nT)}}{1-(1-\gamma)e^{-(\omega+\mu)T}}\right), \frac{\Lambda\gamma e^{-(\omega+\mu)(t-nT)}}{\mu\left(1-(1-\gamma)e^{-(\omega+\mu)T}\right)}, 0, 0, 0, 0\right)$$

for $t \in (nT, (n+1)T], n \in \mathbb{Z}_+$ where

$$\tilde{S}(nT^+) = \tilde{S}(0^+) = \frac{\Lambda}{\mu}\left(1 - \frac{\gamma}{1-(1-\gamma)e^{-(\omega+\mu)T}}\right),$$

and

$$\tilde{V}(nT^+) = \tilde{V}(0^+) = \frac{\Lambda\gamma}{\mu\left(1-(1-\gamma)e^{-(\omega+\mu)T}\right)}.$$

Theorem 4.1. *The disease-free periodic solution* $(\tilde{S}(t), \tilde{V}(t), 0, 0, 0, 0)$ *is locally asymptotically stable if the following condition holds:*

$$(A+B)T > \int_0^T \sqrt{(A-B)^2 + 4\beta\rho\tilde{S}(t)}\, dt. \tag{4.7}$$

The transmission rate must be sufficiently low in order for the property (4.7) *to hold, as stated by*

$$\beta < \beta_c = \frac{AB\mu[1-(1-\gamma)e^{-(\omega+\mu)T}]}{\rho\Lambda(1-e^{-(\omega+\mu)T})}. \tag{4.8}$$

Proof. Let us consider a small perturbation:

$$\begin{aligned} S(t) &= \tilde{S}(t) + u_1(t), \\ V(t) &= \tilde{V}(t) + u_2(t), \\ E(t) &= u_3(t), \\ I(t) &= u_4(t), \\ H(t) &= u_5(t), \\ R(t) &= u_6(t), \end{aligned}$$

from the point $(\tilde{S}(t), \tilde{V}(t), 0, 0, 0, 0)$. Then,

$$\begin{pmatrix} u_1(t) \\ u_2(t) \\ u_3(t) \\ u_4(t) \\ u_5(t) \\ u_6(t) \end{pmatrix} = \Phi(t) \begin{pmatrix} u_1(0) \\ u_2(0) \\ u_3(0) \\ u_4(0) \\ u_5(0) \\ u_6(0) \end{pmatrix}, \quad 0 < t < T,$$

where $\Phi(t)$ satisfies

$$\frac{d\Phi(t)}{dt} = \begin{pmatrix} -\mu & \omega & 0 & -\beta\tilde{S} & 0 & \phi \\ 0 & -(\omega+\mu) & 0 & 0 & 0 & 0 \\ 0 & 0 & -B & \beta\tilde{S} & 0 & 0 \\ 0 & 0 & \rho & -A & 0 & 0 \\ 0 & 0 & 0 & \alpha & -D & 0 \\ 0 & 0 & 0 & q & \kappa & -C \end{pmatrix} \Phi(t).$$

Since the columns of $\Phi(t)$ are particular linearly independent solutions to the initial condition $\Phi(0) = I_6$, the fundamental matrix $\Phi(t) = \Phi(t+T)$ of the six-order differential system which is nonsingular for all time is defined as the monodromy matrix $\Phi(T)$ for any $t = nT$, having the following form:

$$\Phi(T) = Diag\left(e^{-\mu T}, e^{-(\omega+\mu)T}, e^{-CT}, e^{-DT}, \exp\left(\int_0^T J_1(t)\,dt\right), \exp\left(\int_0^T J_2(t)\,dt\right)\right),$$

where

$$J_1(t) = -\frac{1}{2}\left(A + B + \sqrt{(A-B)^2 + 4\beta\rho\tilde{S}(t)}\right); \ \forall t \in [0, T],$$

$$J_2(t) = -\frac{1}{2}\left(A + B - \sqrt{(A-B)^2 + 4\beta\rho\tilde{S}(t)}\right); \ \forall t \in [0, T].$$

Linearization of Eq (2.2) yields

$$\begin{pmatrix} u_1(nT^+) \\ u_2(nT^+) \\ u_3(nT^+) \\ u_4(nT^+) \\ u_5(nT^+) \\ u_6(nT^+) \end{pmatrix} = \begin{pmatrix} 1-\gamma & 0 & 0 & 0 & 0 & 0 \\ \gamma & 1 & 0 & 0 & 0 & 0 \\ 0 & 0 & 1 & 0 & 0 & 0 \\ 0 & 0 & 0 & 1 & 0 & 0 \\ 0 & 0 & 0 & 0 & 1 & 0 \\ 0 & 0 & 0 & 0 & 0 & 1 \end{pmatrix} \begin{pmatrix} u_1(nT) \\ u_2(nT) \\ u_3(nT) \\ u_4(nT) \\ u_5(nT) \\ u_6(nT) \end{pmatrix}.$$

According to Floquet theory, the solution $(\tilde{S}(t), \tilde{V}(t), 0, 0, 0, 0)$ is locally stable if the modulus of all eigenvalues of K is less than 1 when K is defined by

$$K = \begin{pmatrix} 1-\gamma & 0 & 0 & 0 & 0 & 0 \\ \gamma & 1 & 0 & 0 & 0 & 0 \\ 0 & 0 & 1 & 0 & 0 & 0 \\ 0 & 0 & 0 & 1 & 0 & 0 \\ 0 & 0 & 0 & 0 & 1 & 0 \\ 0 & 0 & 0 & 0 & 0 & 1 \end{pmatrix} \Phi(T).$$

Note that the eigenvalues of K are given by

$$\psi_1 = (1-\gamma)\exp(-\mu T),$$
$$\psi_2 = \exp(-(\omega+\mu)T),$$
$$\psi_3 = \exp(-CT),$$
$$\psi_4 = \exp(-DT),$$

$$\psi_5 = \exp\left(\int_0^T -\frac{1}{2}\left(A+B+\sqrt{(A-B)^2+4\beta\rho\tilde{S}(t)}\right)dt\right),$$
$$\psi_6 = \exp\left(\int_0^T -\frac{1}{2}\left(A+B-\sqrt{(A-B)^2+4\beta\rho\tilde{S}(t)}\right)dt\right).$$

Since Eq (4.7) holds, the modulus of all eigenvalues is less than 1, indicating local asymptotic stability for sufficiently small initial conditions. Additionally, for Eq (4.8) to hold, it is necessary that

$$(A+B)^2 > (A-B)^2 + 4\beta\rho \max_{t\in[0,T]} \tilde{S}(t)$$

which is satisfied if Eq (4.8) holds.

5. Numerical simulations

We proceed to assess the SEIR and SVEIHR models through numerical simulations. The model system has been implemented by using MATLAB, utilizing packages such as ode45 to solve ordinary differential equations, optimvar to optimize parameter values, fcn2optimexpr to translate functions into optimization expressions, and ode15s to address impulsive differential equations.

Our numerical evaluations are conducted by using initial values sourced from the USA data, as provided by the WHO website [3]. Additionally, we utilized the parameter values outlined in Table 1 for our simulations.

$$S(0) = 338,173,377, V(0) = 10,000, E(0) = 10,000, I(0) = 56,029, H(0) = 40,450,$$

$$\text{and } R(0) = 10,000.$$

A computer simulation of the system (3.1) is presented in Figure 2, utilizing the parameter values specified in Table 1. The transmission rate (β) has been increased by two times, resulting in $R_0 = 2.3307 > 1$. In accordance with Theorem 3.4, the solution trajectory clearly indicates a convergence toward the endemic equilibrium (EE^*), as demonstrated by the model's dynamics.

If the rate of transitioning from infected individuals to hospitalization increases by 40% (i.e., α increases by 40%), the basic reproduction number will decrease, resulting in $R_0 = 0.8633 < 1$, as illustrated in Figure 3. In accordance with Theorem 3.3, the solution trajectory leads to the disease-free equilibrium (EE).

Table 1. Parameter values.

Parameter	Value	Source	Unit
$S(0)$	338,173,377	WHO [3]	Individuals
$V(0)$	10,000	Assumed	Individuals
$E(0)$	10,000	Assumed	Individuals
$I(0)$	56,029	WHO [3]	Individuals
$H(0)$	40,450	WHO [3]	Individuals
$R(0)$	10,000	Assumed	Individuals
Λ	3251	Calculated	Individuals $\times$ Day^{-1}
β	9.1508×10^{-9}	Calculated* [33]	Individuals^{-1} $\times$ Day^{-1}
μ	0.3349×10^{-4}	[33]	Day^{-1}
ϕ	0.0426	Fitting	Day^{-1}
ρ	1/4.2	[23]	Day^{-1}
q	1/30	[11]	Day^{-1}
δ_1	1/16.1	[23]	Day^{-1}
δ_2	1/11.2	[23]	Day^{-1}
α	1/1.5	[23]	Day^{-1}
κ	1/11.5	[23]	Day^{-1}

* The value is calculated by dividing the transmission rate by the total population when the system is in equilibrium.

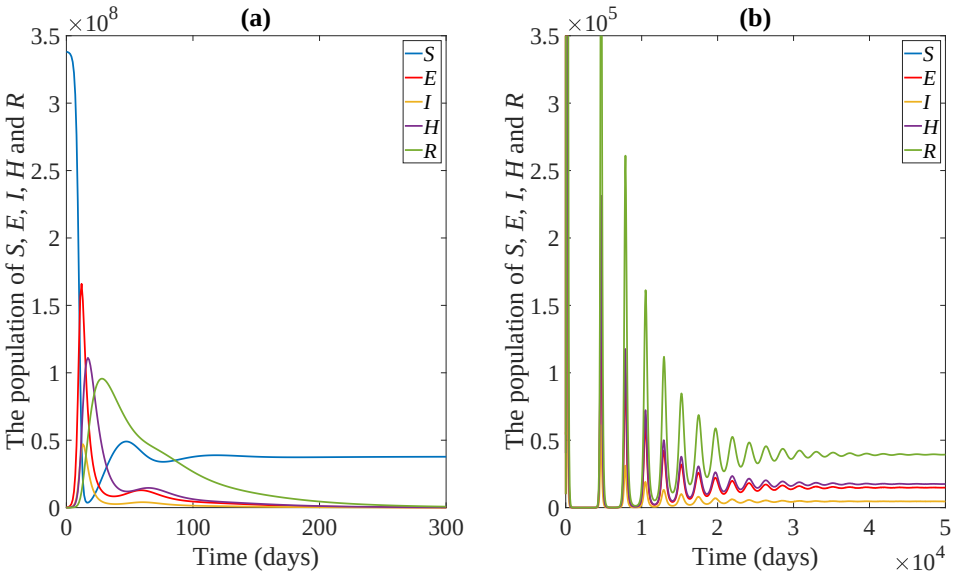

Figure 2. (a) Time series of the susceptible population (S), exposed population (E), infected population (I), hospitalized population (H), and the recovered population (R). The solution trajectory tends toward the endemic equilibrium (EE^*) when the basic reproduction number $R_0 > 1$. (b) Zoom-in of (a), highlighting specific trends in the population dynamics.

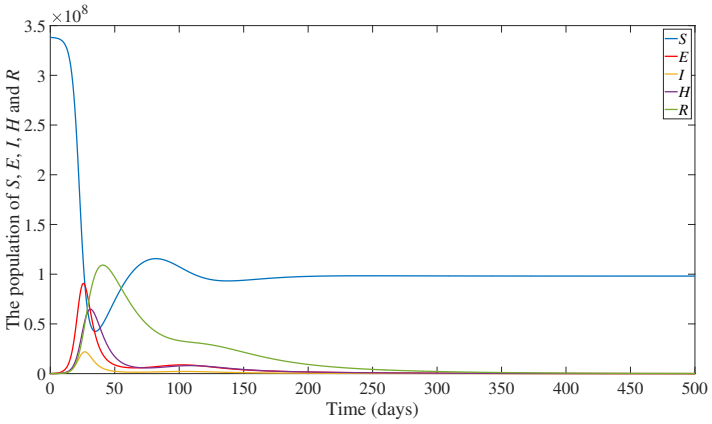

Figure 3. The time series of the susceptible population (S), exposed population (E), infected population (I), hospitalized population (H), and the recovered population (R). The solution trajectory demonstrates a tendency toward the disease-free equilibrium (EE) when the basic reproduction number $R_0 < 1$.

5.1. The case study

In this section, we discuss the numerical simulations of the model system (3.1), the parameters of which were fitted by using ode45, optimvar, and fcn2optimexpr in MATLAB. These simulations have yielded the parameter set summarized in Table 2. Our primary objective here is to present a comparative analysis between the simulated results and empirical data, focusing our attention on two crucial epidemiological indicators: the count of infectious individuals and the count of hospitalized individuals. The empirical data used for this comparative analysis were obtained from the WHO website, drawing upon data specific to the USA [3]. These real-world observations pertain to confirmed cases of infection, collected through COVID-19 swab tests. Commencing on January 1, 2023, the data collection extended over a span of 138 days, as illustrated in Figures 4 through 5.

Table 2. Fitting and calulation of parameter values.

Parameter	Value	Source	Unit
Λ	3251	Calculated	Individuals $\times$ Day^{-1}
β	0.0001	Fitting	Individuals^{-1} $\times$ Day^{-1}
μ	0.0136	Fitting	Day^{-1}
ϕ	0.0426	Fitting	Day^{-1}
ρ	0.0001	Fitting	Day^{-1}
q	0.0848	Fitting	Day^{-1}
δ_1	0.0034	Fitting	Day^{-1}
δ_2	0.2996	Fitting	Day^{-1}
α	0.4272	Fitting	Day^{-1}
κ	0.3852	Fitting	Day^{-1}

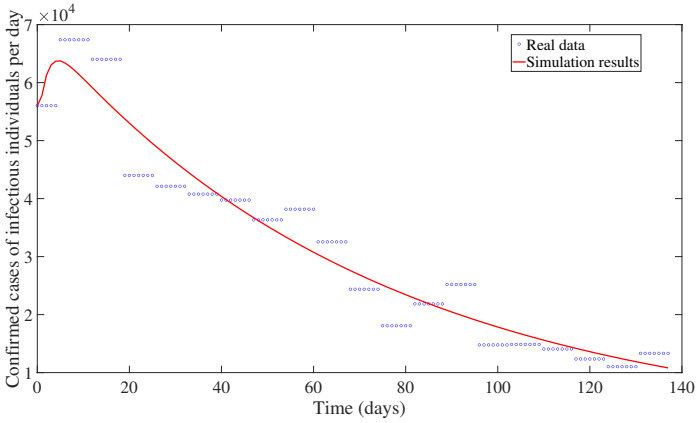

Figure 4. The number of confirmed cases of infectious individuals per day.

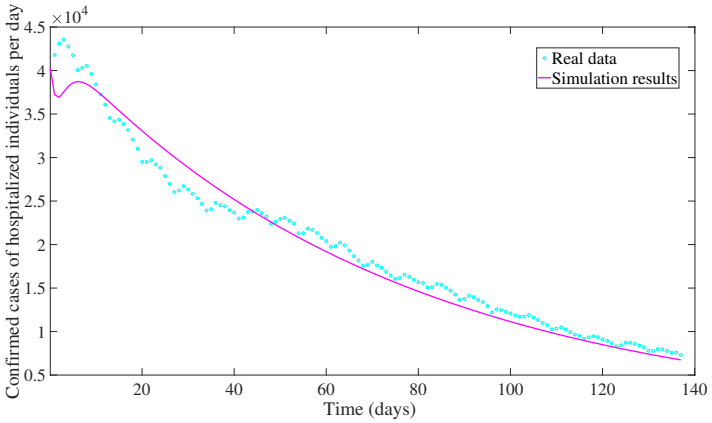

Figure 5. The number of confirmed cases of hospitalized individuals per day.

The confirmed cases for the infectious class, as simulated by the model (red solid line), fit the reported COVID-19 case data (blue circle) with $R^2 = 0.932$, showing that the model fits well in Figure 4. According to Figure 5, the verified cases of the hospitalized class simulated by using the model (pink solid line) are quite similar to the true data (light blue circle), with $R^2 = 0.970$.

5.2. The simulation of the impulsive vaccination

One starts by considering an impulsive vaccination with the parameters of vaccination proportion and impulse period ($\gamma = 0.9$, $T = 90$ days) while varying a low vaccine immunity rate ω. Figure 6 illustrates the development over time. Theorem 4.1 predicts that the evolution will eventually lead to a periodic solution, which is what has been shown to occur.

Figures 7 and 8 display the results for $T = 90$ days as γ varies and $\gamma = 0.5$ as T varies, respectively. It can be seen that the exposed, infected, and hospitalized populations decrease as γ increases and as T is reduced, as would be predicted theoretically.

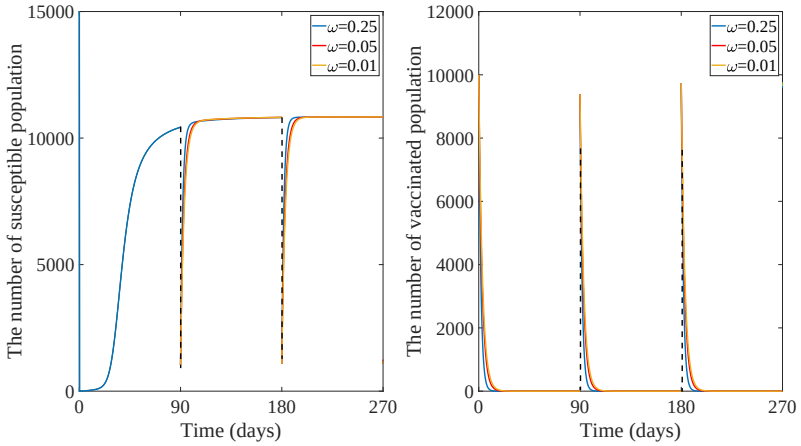

Figure 6. Evolution of susceptible and vaccinated populations under impulsive vaccination with $\gamma = 0.9$, $T = 90$ days as ω varies.

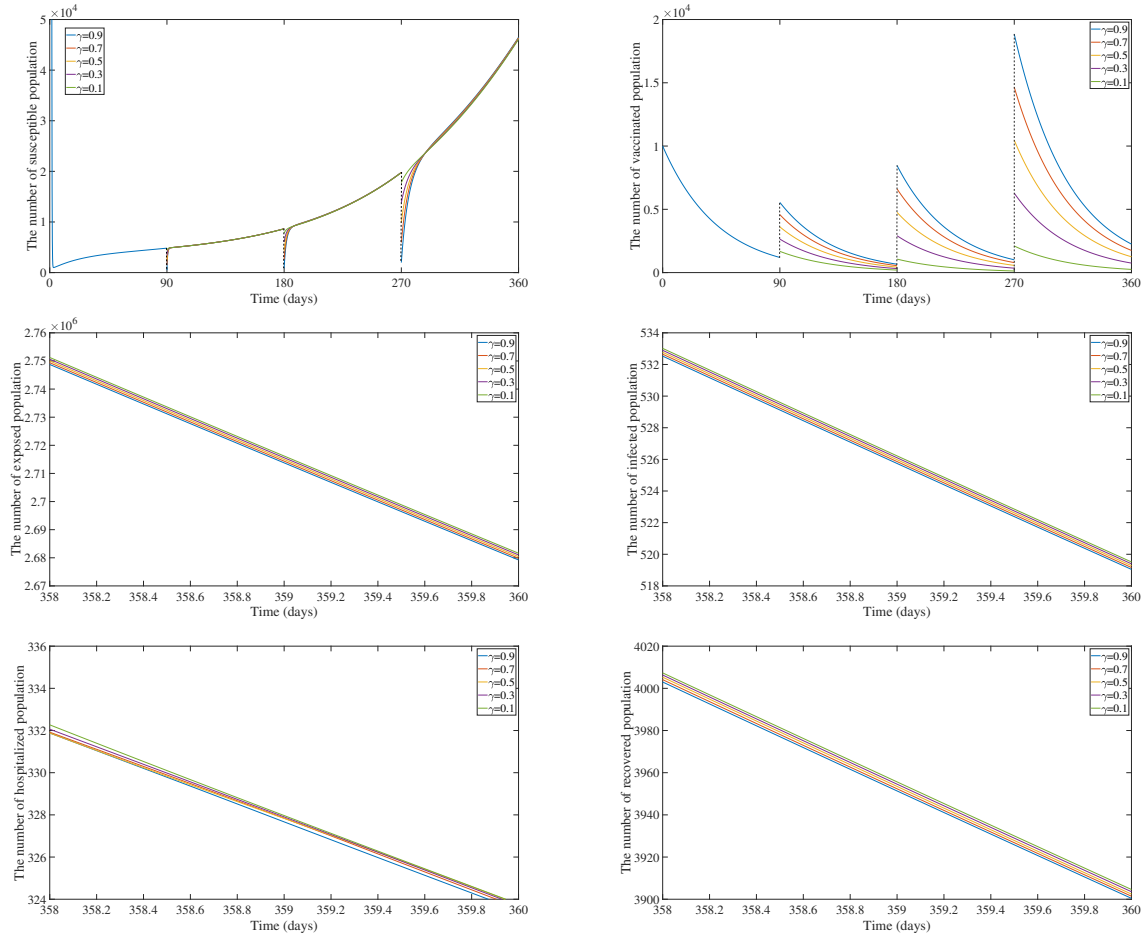

Figure 7. Comparison of the susceptible, vaccinated, exposed, infected, hospitalized, and recovered populations for $T = 90$ days as γ varies.

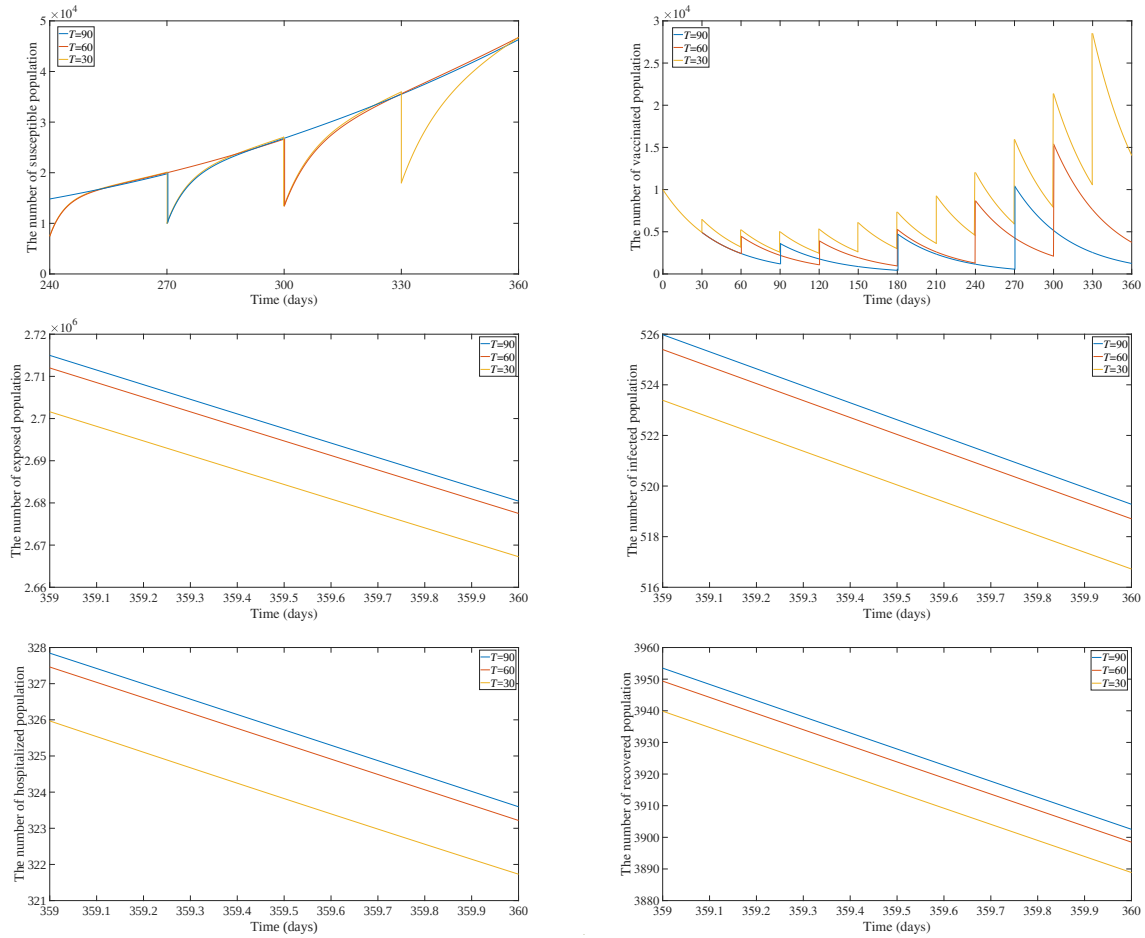

Figure 8. Comparison of the susceptible, vaccinated, exposed, infected, hospitalized, and recovered populations for $\gamma = 0.5$ as T varies.

Figure 9 presents a comprehensive view of the susceptible, exposed, infected, hospitalized, and recovered populations, contrasting scenarios with and without the presence of impulsive vaccination. The outcomes discerned from these simulations reveal that, in the case of impulsive vaccination, the disease within the system was effectively eradicated by the 270th day. In stark contrast, the system lacking impulsive vaccination witnessed the disease's containment occurring later, specifically, on the 312th day.

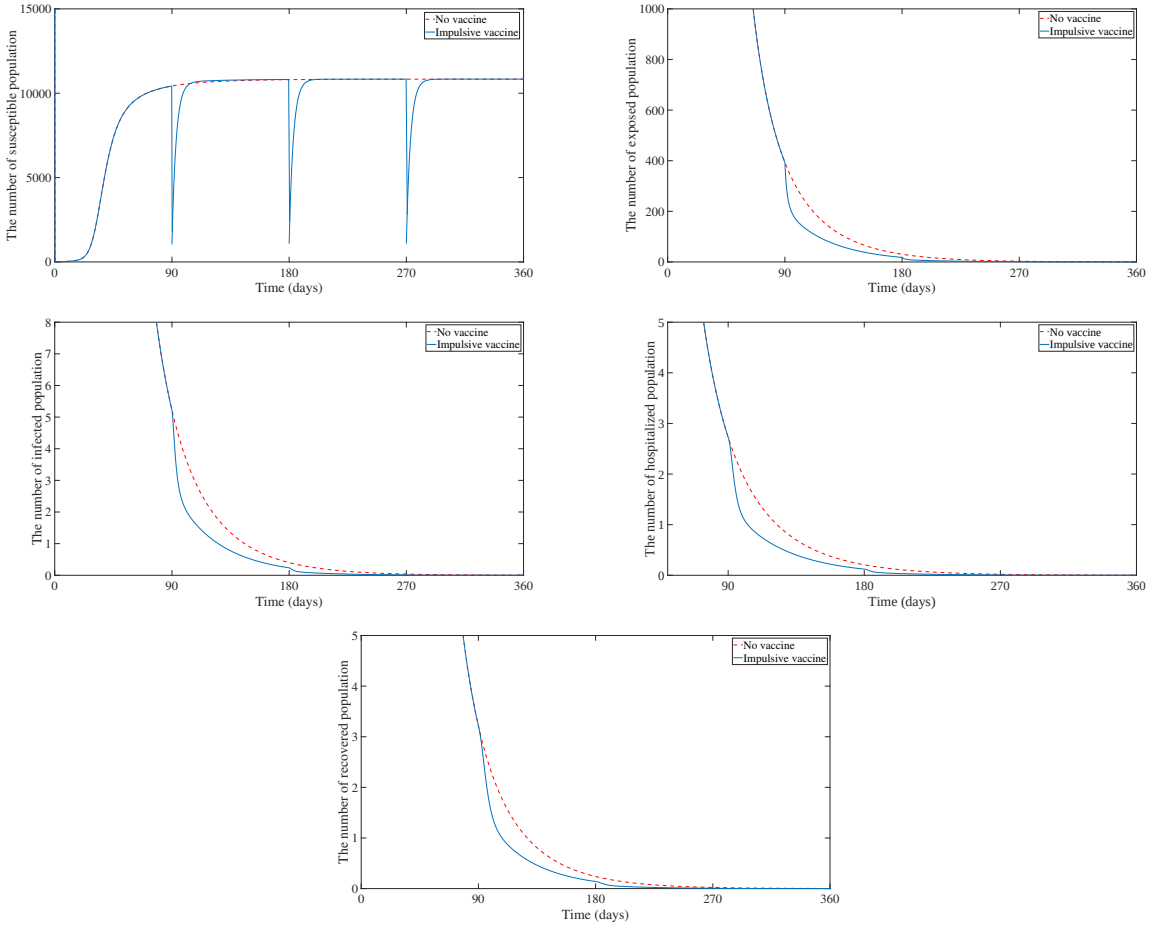

Figure 9. Comparison of the susceptible, exposed, infected, hospitalized, and recovered populations with and without impulsive vaccination ($\gamma = 0.9$, $T = 90$ days, and $\omega = 0.01$).

6. Discussion

In this work, we focus on assessing the impact of impulsive vaccination on the timeline of COVID-19 eradication within the SEIHR epidemic model. Despite the positive findings indicating accelerated disease eradication, it is crucial to acknowledge potential limitations that may influence the study's applicability and scope.

Our analysis suggests that impulsive vaccination can reduce the basic reproduction number, expediting the transition from endemic to disease-free status. However, it is important to note potential limitations, such as variations in vaccine effectiveness over time. These factors could influence the real-world outcomes of impulsive vaccination strategies.

The key observation from our findings is that the implementation of periodic impulsive vaccination efforts significantly shortens the time required to eliminate COVID-19 from a given population. While this is promising, the study's reliance on mathematical modeling and assumptions about population dynamics introduces uncertainties. The applicability of our results to diverse populations and evolving viral strains warrants careful consideration.

Our study highlights the dynamic nature of vaccination campaigns, emphasizing that strategic vaccination efforts can expedite disease eradication. However, we must acknowledge that the success of impulsive vaccination strategies depends on several external factors, including public compliance, infrastructure, and evolving epidemiological conditions.

7. Conclusions

This study explored the dynamics of COVID-19 transmission and the potential impact of impulsive vaccination strategies. We began by investigating the stability of disease-free equilibrium and determined the basic reproduction number (R_0) to be a critical parameter influencing disease spread. Utilizing mathematical methods and numerical simulations, we examined the SEIR and SVEIHR models, implementing parameter estimation techniques to align our models with real-world data.

Our numerical simulations, based on data from the WHO, allowed us to compare model predictions with actual observations. We specifically concentrated on the amount of infected and hospitalized people, offering valuable insights into the effectiveness of impulsive vaccination in controlling the disease. Notably, our results have demonstrated that impulsive vaccination strategies could lead to a quicker containment of the disease compared to scenarios without such interventions.

This research contributes to the understanding of COVID-19 dynamics and emphasizes the potential benefits of strategic vaccination approaches. These findings underscore the importance of vaccination campaigns in disease control and public health efforts, particularly in the face of evolving viral threats.

In summation, this research contributes valuable insights into the dynamics of SEIR epidemiological models with newborns and impulsive vaccination. The findings underscore the significance of vaccination efforts, yet we must interpret these results cautiously due to the study's simplifications and assumptions. Recognizing these limitations is crucial for a comprehensive understanding of the study's scope and potential implications for real-world public health strategies, especially in the context of emerging infectious diseases like COVID-19.

Use of AI tools declaration

The authors declare that they have not used artificial intelligence tools in the creation of this article.

Acknowledgments

I. C. was supported by the Office of the Permanent Secretary, Ministry of Higher Education, Science, Research and Innovation (OPS MHESI) (Grant No. RGNS 64-139), Thailand Science Research and Innovation (TSRI) and Mahasarakham University. C. R. was supported by the NSRF via the Program Management Unit for Human Resources & Institutional Development, Research and Innovation (Grant No. B05F640231), and the Centre of Excellence in Mathematics, Thailand.

Conflict of interest

The authors declare no conflict of interest.

References

1. Coronavirus disease 2019 (covid-19): Situation report-126, 2020. Available from: https://www.who.int/publications/m/item/situation-report---126.
2. Nebraska Medicine, Covid-19: Disease-induced (natural) immunity, vaccination or hybrid immunity? 2023. Available from: https://www.nebraskamed.com/COVID/covid-19-studies-natural-immunity-versus\-vaccination.
3. WHO COVID-19 dashboard data, 2020. Available from: https://data.who.int/dashboards/covid19/data?n=c.
4. I. Alazman, K. S. Albalawi, P. Goswami, K. Malik, A restricted sir model with vaccination effect for the epidemic outbreaks concerning covid-19, *CMES-Comp. Model. Eng.*, **137** (2023), 3. https://doi.org/10.32604/cmes.2023.028674
5. C. Anastassopoulou, L. Russo, A. Tsakris, C. Siettos, Data-based analysis, modelling and forecasting of the covid-19 outbreak, *PloS one*, **15** (2020), e0230405. https://doi.org/10.1371/journal.pone.0230405
6. R. M. Anderson, R. M. May, *Infectious diseases of humans: Dynamics and control*, Oxford university press, 1991.
7. G. Ballinger, X. Liu, Permanence of population growth models with impulsive effects, *Math. Comput. Model.*, **26** (1997), 59–72. https://doi.org/10.1016/S0895-7177(97)00240-9
8. F. Brauer, C. Castillo-Chavez, C. Castillo-Chavez, *Mathematical models in population biology and epidemiology*, New York: Springer, 2012.
9. F. Casella, Can the covid-19 epidemic be controlled on the basis of daily test reports? *IEEE Control Syst. Lett.*, **5** (2021), 1079–1084. https://doi.org/10.1109/LCSYS.2020.3009912
10. C. Chiyaka, W. Garira, S. Dube, Transmission model of endemic human malaria in a partially immune population, *Math. Comput. Model.*, **46** (2007), 806–822. https://doi.org/10.1016/j.mcm.2006.12.010
11. C. A. Ciro, S. A. James, H. McGuire, V. Lepak, S. Dresser, A. Costner-Lark, et al., Natural, longitudinal recovery of adults with covid-19 using standardized rehabilitation measures, *Front. Aging Neurosci.*, **14** (2022), 958744. https://doi.org/10.3389/fnagi.2022.958744
12. M. F. Danca, N. Kuznetsov, Matlab code for lyapunov exponents of fractional-order systems, *Int. J. Bifurcat. Chaos*, **28** (2018), 1850067. https://doi.org/10.1142/S0218127418500670
13. W. R. Derrick, S. I. Grossman, *Elementary differential equations with applications*, Addision Wesley Publishing Company, 1976.
14. O. Diekmann, J. A. P. Heesterbeek, *Mathematical epidemiology of infectious diseases: Model building, analysis and interpretation*, John Wiley & Sons, 2000.
15. M. Etxeberria-Etxaniz, S. Alonso-Quesada, M. De la Sen, On an seir epidemic model with vaccination of newborns and periodic impulsive vaccination with eventual on-line adapted vaccination strategies to the varying levels of the susceptible subpopulation, *Appl. Sci.*, **10** (2020), 8296. https://doi.org/10.3390/app10228296

16. H. Gaff, E. Schaefer, Optimal control applied to vaccination and treatment strategies for various epidemiological models, *Math. Biosci. Eng.*, **6** (2009), 469–492. https://doi.org/10.3934/mbe.2009.6.469

17. W. O. Kermack, A. G. McKendrick, A contribution to the mathematical theory of epidemics, *Proc. R. Soc. Lond. A*, **115** (1927), 700–721. https://doi.org/10.1098/rspa.1927.0118

18. K. Kuga, J. Tanimoto, Which is more effective for suppressing an infectious disease: Imperfect vaccination or defense against contagion? *J. Stat. Mech.*, **2018** (2018), 023407. https://doi.org/10.1088/1742-5468/aaac3c

19. J. P. La Salle, *The stability of dynamical systems*, Society for Industrial and Applied Mathematics, 1976.

20. V. Lakshmikantham, P. S. Simeonov, *Theory of impulsive differential equations*, World scientific, 1989.

21. Q. Lin, S. Zhao, D. Gao, Y. Lou, S. Yang, S. S. Musa, et al., A conceptual model for the coronavirus disease 2019 (covid-19) outbreak in wuhan, china with individual reaction and governmental action, *Int. J. Infect. Dis.*, **93** (2020), 211–216. https://doi.org/10.1016/j.ijid.2020.02.058

22. H. Park, S. H. Kim, A study on herd immunity of covid-19 in south korea: Using a stochastic economic-epidemiological model, *Environ. Resource Econ.*, **76** (2020), 665–670. https://doi.org/10.1007/s10640-020-00439-8

23. S. Sanche, Y. T. Lin, C. Xu, E. Romero-Severson, N. Hengartner, R. Ke, High contagiousness and rapid spread of severe acute respiratory syndrome coronavirus 2, *Emerg. Infect. Dis.*, **26** (2020), 1470. https://doi.org/10.3201/eid2607.200282

24. A. K. Singh, M. Mehra, S. Gulyani, A modified variable-order fractional sir model to predict the spread of covid-19 in india, *Math. Method. Appl. Sci.*, 2021. https://doi.org/10.1002/mma.7655

25. N. Sweilam, S. Al-Mekhlafi, D. Baleanu, Optimal control for a fractional tuberculosis infection model including the impact of diabetes and resistant strains, *J. Adv. Res.*, **17** (2019), 125–137. https://doi.org/10.1016/j.jare.2019.01.007

26. N. Sweilam, S. AL-Mekhlafi, Optimal control for a nonlinear mathematical model of tumor under immune suppression: A numerical approach, *Optim. Contr. Appl. Met.*, **39** (2018), 1581–1596. https://doi.org/10.1002/oca.2427

27. N. Sweilam, O. Saad, D. Mohamed, Fractional optimal control in transmission dynamics of west nile virus model with state and control time delay: A numerical approach, *Adv. Differ. Equ.*, **2019** (2019), 210. https://doi.org/10.1186/s13662-019-2147-8

28. N. Sweilam, O. Saad, D. Mohamed, Numerical treatments of the tranmission dynamics of west nile virus and it's optimal control, *Electon. J. Math. Anal. Appl.*, **7** (2019), 9–38.

29. J. Tanimoto, *Sociophysics approach to epidemics*, Singapore: Springer, 2021.

30. P. van den Driessche, J. Watmough, Reproduction numbers and sub-threshold endemic equilibria for compartmental models of disease transmission, *Math. Biosci.*, **180** (2002), 29–48. https://doi.org/10.1016/S0025-5564(02)00108-6

31. T. P. Velavan, C. G. Meyer, The covid-19 epidemic, *Trop. Med. Int. Health*, **25** (2020), 278–280. https://doi.org/10.1111/tmi.13383

32. J. T. Wu, K. Leung, M. Bushman, N. Kishore, R. Niehus, P. M. de Salazar, et al., Estimating clinical severity of covid-19 from the transmission dynamics in wuhan, china, *Nat. Med.*, **26** (2020), 506–510. https://doi.org/10.1038/s41591-020-0822-7

33. B. Yang, Z. Yu, Y. Cai, The impact of vaccination on the spread of covid-19: Studying by a mathematical model, *Physica A*, **590** (2022), 126717. https://doi.org/10.1016/j.physa.2021.126717

AIMS Press

© 2024 the Author(s), licensee AIMS Press. This is an open access article distributed under the terms of the Creative Commons Attribution License (http://creativecommons.org/licenses/by/4.0)